BIODIVERSITAS
Volume 25, Number 3, March 2024
Pages: 1104-1115

ISSN: 1412-033X
E-ISSN: 2085-4722
DOI: 10.13057/biodiv/d250325

Distribution and FTIR-based fingerprint of secondary metabolites in different organs of ant-plant (*Myrmecodia tuberosa*)

NIYA BUDHI LESTARI[1], YOHANA C. SULISTYANINGSIH[2], ABDUL HALIM UMAR[3], DIAH RATNADEWI[2,♥]

[1]Plant Biology Graduate Program, Department of Biology, Faculty of Mathematics and Natural Sciences, Institut Pertanian Bogor. Jl. Agatis, IPB Darmaga Campus, Bogor 16680, West Java, Indonesia

[2]Department of Biology, Faculty of Mathematics and Natural Sciences, Institut Pertanian Bogor. Jl. Agatis, IPB Darmaga Campus, Bogor 16680, West Java, Indonesia. Tel/fax.: +6281316317211, ♥email: dratnadewi@apps.ipb.ac.id

[3]College of Pharmaceutical Sciences Makassar, Sekolah Tinggi Ilmu Farmasi Makassar. Jl. Perintis Kemerdekaan Km. 13.7, Makassar 90242, South Sulawesi, Indonesia

Manuscript received: 20 June 2023. Revision accepted: 23 March 2024.

Abstract. *Lestari NB, Sulistyaningsih YC, Umar AH, Ratnadewi D. 2024. Distribution and FTIR-based fingerprint of secondary metabolites in different organs of ant-plant* (Myrmecodia tuberosa). *Biodiversitas 25: 1104-1115. Myrmecodia tuberosa* Jack, or ant-plant, is widely used as a traditional medicine. The plant has the potential to be antimicrobial, anticancer, and antioxidant. Its domatium is believed to contain valuable substances, rendering people to collect the organ that devastates the whole plant. Therefore, the distribution and nature of the major substances in the leaf, petiole, and domatium must be investigated. This study aimed to determine the secondary metabolites and their accumulation sites through anatomy and histochemistry. Fourier-transform infrared (FTIR) and chemometrics supported the determination. Microscopic preparations made observations of the anatomy and secretory structures of transverse and paradermal sections. Histochemical studies were performed with specific reagents. *M. tuberosa* has a hypostomatic leaf blade with parasitic stomata. The main secretory structure is the idioblast. Idioblasts are scattered over various tissues, such as the epidermis, hypodermis, palisade, spongy mesophyll, and cuticle of the leaf blade, in the epidermal tissue, chlorenchyma cortex, and cuticle of petiole and the periderm, cortex, and pith of domatium. Terpenoids, phenols, lipophilic compounds, essential oils, and flavonoids were found in the leaf blade, petiole, and domatium, whereas alkaloids were present only in the petioles. FTIR demonstrated the main functional groups in the three organs are similar, while the principal component analysis distinguished domatium from leaf blade and petiole.

Keywords: Chemometrics, domatium, FTIR spectra, idioblast, secretory structure

INTRODUCTION

Indonesia has a mega-diversity of medicinal plants. At least 80% of medicinal plant species in Southeast Asia are found in Indonesia (Cahyaningsih et al. 2021). The plant families widely used as medicinal ingredients include Zingiberaceae, Asteraceae, Fabaceae, and Rubiaceae (Utami et al. 2019; Silalahi et al. 2021). *Myrmecodia tuberosa* Jack, or ant-plant, was named according to the Australian Plant Census (APC) (CHAH 2011). It is a member of Rubiaceae. *Myrmecodia* is an epiphytic plant that has a modified swollen stem (domatium) that looks like a tuber (Greenfield et al. 2021); inside the domatium, some cavities are inhabited by ants, mostly *Iridomyrmex cordatus* (Huxley 1978). *Myrmecodia* disperses in the Malaysian Peninsula, the Philippines, Papua New Guinea, Cape York, the Solomon Islands, and Indonesia (Huxley and Jebb 1993).

The local people of Sumatra, Papua, and Sulawesi used the ant-plant as a traditional medicinal ingredient to cure several diseases, such as tumors, cancer, and muscle pain, and enhance the body's immunity (Mardany et al. 2016; Indra et al. 2019). The ethanol extract of *M. tuberosa* domatium has been shown to reduce tumor growth (Yuletnawati et al. 2016), has the potential as an antimicrobial (Efendi and Hertiani 2012), antioxidant, and antidiabetic (Rasemi et al. 2014). Its medicinal effects are gained from its variety of secondary metabolites. Plants producing secondary metabolites synthesize a variety of unique bioactive compounds. The leaf blade of *M. tuberosa* contained flavonoids, phenols, alkaloids, and steroids, while the domatium contained flavonoids, phenols, alkaloids, and triterpenoids (Sari et al. 2017). Plant secondary metabolites are generally accumulated in specialized structures called secretory structures (Lange 2015). Each part of a plant has a different distribution and types of secondary metabolite (Nurhasanah and Iriani 2021; Umar et al. 2021a). The anatomical characteristics and secretory structures of medicinal plants need to be validated to ensure authenticity and identify the highest accumulation of a bioactive substance (Coelho et al. 2012). Histochemical tests were conducted to see the distribution and accumulation of secondary metabolites and types of secretory structures found in plants.

Fingerprint profile analysis with Fourier Transform Infrared (FTIR) Spectroscopy is frequently carried out to see whether there are differences in functional chemical groups among plant organs or species. FTIR is simpler, can perform measurements quickly, and can analyze several components simultaneously. The resulting data, in the form

of an FTIR spectrum, are very complex and challenging to interpret. Therefore, the further chemometric analysis uses principle component analysis (PCA). The combination of FTIR spectra with chemometrics has been widely applied, as demonstrated by Yudthavorasit et al. (2014), to identify and authenticate two different ginger species and by Umar et al. (2021b) in two species of *Curculigo*.

Research on phytochemistry, antioxidant and anti-diabetes activities, and the potential of ant-plant as an anticancer have previously been carried out. Still, information on the accumulation of secondary metabolites, secretory structure, and functional chemical groups of secondary metabolites of ant-plant, especially the species *M. tuberosa*, has never been reported. Therefore, this study determined the anatomy, types, and distribution of secretory structures, the main groups of secondary metabolites qualitatively, and the functional chemical groups contained in the leaf blade, petiole, and domatium of *M. tuberosa* to know the richness and composition of secondary metabolites in each of the three organs.

MATERIALS AND METHODS

Plant materials

A sampling of *M. tuberosa* Jack was carried out in Ogowele Village (0º42'19.15"N, 120º24'09.60"E), Dondo Sub-district, Tolitoli District, Central Sulawesi (Figure 1). The plant samples have reached adulthood, marked by the reproductive organs as flowers or fruits. The parts observed included the leaf blade, petiole, and domatium. Three sample replicates of the leaf blade, petiole, and domatium were collected from three plants. The plant identification was carried out at the National Research and Innovation Agency (BRIN) Indonesia, with the herbarium voucher number BO-1318722.

Observation of anatomical structures

The microscopic sample was prepared by transverse and paradermal incisions on the leaf blade, petiole, and domatium, following the method described by Sass (1951). The leaf, petiole, and domatium were slashed crosswise using a razor blade, stained with 1% safranin or distilled water, and then covered with a cover glass. The adaxial or abaxial part of the leaf, which had been fixed with 70% alcohol, was paradermally incised using a razor blade to observe stomata. The samples were observed under an Olympus CX33 compound microscope, followed by taking pictures using Indomicro Viewer® ver.3.7.

Histochemical test and secretory structure observation

The histochemical test was carried out using a fresh sample. Transversal sections of the leaf blade, petiole, and domatium were made manually using a razor blade. Transversal sections of the sample tissues were tested by immersing them in a specific reagent, and then the color change was observed. Phenolic compounds were identified with 10% ferric chloride reagent (Merck, Darmstadt, Germany), then a few grains of sodium carbonate (Merck, Darmstadt, Germany) were added. The samples were immersed in 1 mL of reagent for 30 minutes, after which the samples were observed under a light microscope. A positive reaction was indicated by a black or green color (Johansen 1940).

Flavonoids were identified using 5% aluminum chloride reagent (Merck, Darmstadt, Germany) in 85% alcohol (Merck, Darmstadt, Germany)] for 30 minutes, then observed under a fluorescent microscope with a UV filter. The presence of flavonoids was indicated by a yellow glow (flavonols), greenish yellow (flavones), or blue (flavanones) (Guerin et al. 1971).

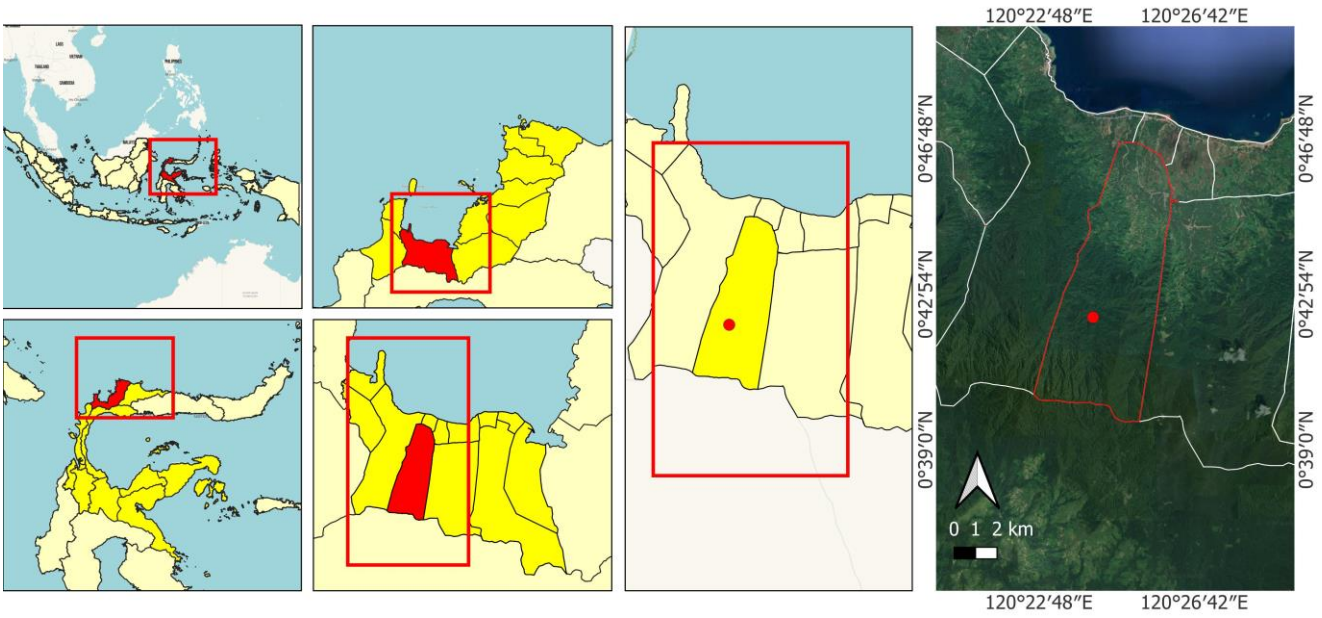

Figure 1. Location of Ogowele Village, Dondo, Central Sulawesi, indicating the sampling sites of *Myrmecodia tuberosa* (*red dot*)

Essential oils and terpenes were detected by NADI reagent [α-naphtol (Merck & Co., Darmstadt, Germany) and N,N-dimethyl-p-phenylendiamine (Fujifilm Wako Chemistry, Osaka, Japan)]. The sample was placed for 20 minutes in a freshly prepared reagent (David and Carde 1964). Purple indicated terpenes, and blue was confirmed for essential oils. To reconfirm the presence of terpenoid compounds, we also use 5% cupric acetate (Merck, Darmstadt, Germany). The sample was placed for 30 minutes in a freshly prepared reagent and then observed under a light microscope. Positive results gave reddish-brown or brownish-yellow color on the tissue (Martin et al. 2002).

Lipophilic compounds were tested in 70% alcohol (Merck, Darmstadt, Germany) for 1 minute, then in 0.03% Sudan IV (Merck, Darmstadt, Germany) in alcohol 70% (Merck, Darmstadt, Germany). The samples were immersed in 1 mL of reagent for 30 minutes, after which the samples were observed under a light microscope. Positive results (of lipids, triglycerides, and lipoprotein) were obtained when red, yellow or orange color appeared (Boix et al. 2011).

Alkaloid compounds were tested in Wagner reagent [(1 g iodin powder (Merck, Darmstadt, Germany), 1 g potassium iodide powder (Merck, Darmstadt, Germany), dissolved in 100 mL of aquadest (Merck, Darmstadt, Germany)]. A reddish-brown color indicated a positive reaction. As a negative control, some other tissue samples were soaked in a 5% tartaric acid solution in 95% alcohol for 48 hours before being treated with the reagent, then observed under a light microscope (Furr and Mahlberg 1981).

Sample extraction and FTIR analysis

Samples obtained from the field were washed in tap water, then chopped into small pieces, and dried at 40 °C in an oven for 1-2 days. The dried samples were ground in a grinder. The extraction referred to the method developed by Indra et al. (2019). As much as 10 g of dry powder was soaked in 100 mL of 96% ethanol for 48 hours and stirred occasionally. The extract was filtered through a Whatman paper no. 41, the filtrate was then concentrated using a rotary evaporator at 60 °C. The extract obtained was ready for FTIR analysis.

The analytical method referred to that described by Rafi et al. (2021). A 2 mg sample extract was mixed with 200 mg of KBr and pressed into the disc manually for 10 minutes. The disc was placed in an FTIR Tensor 37 spectrophotometer (Bruker Optik GmBH, Ettlingen, Germany). Deuterated triglycine sulfate (DTGS) was used as a detector. FTIR measurements were carried out in the 4000-400 cm^{-1} region at 4 cm^{-1} resolution, with 32 screens operated with OPUS software version 4.2 (Bruker Optik GmbH, Karlsruhe, Germany).

Antioxidant determination

The antioxidant capacity of the samples was determined by the DPPH method described by Salazar-Aranda et al. (2009). As much as 100 µL (100 ppm) of the sample or ascorbic acid (the standard) was mixed with 100 µL DPPH 125 µM, and let in the dark at 37 °C for 30 minutes. The tests were done in triplicate. A microplate reader was adjusted to 517 nm to read the absorbance. The following equation calculated the scavenging effect:

$$\%\text{scavenging} = \left(\frac{\text{Absorbance of control} - \text{Absorbance of sample}}{\text{Absorbance of control}}\right) x\ 100\%$$

The IC_{50} of samples was plotted on a curve of a series of six different concentrations of DPPH (control). Ethanol served as the blank control.

Data analysis

The processed wavenumber data from FTIR analysis were analyzed using OriginPro software (https://www.originlab.com/getstarted) to see the differences in the chromatogram of each leaf blade, petiole, and domatium sample. PCA analysis using MetaboAnalyst 5.0 (https://www.metaboanalyst.ca/) was performed to determine the grouping pattern of sample extracts using absorbance data in the given wave number range. The IC_{50} data were processed by ANOVA and further by the Duncan Multiple Range Test (DMRT) at α=5%. PLS-DA (partial least squares-discrimination analysis) was employed to identify the correlation between the functional group and its antioxidant activity.

RESULTS AND DISCUSSION

Anatomical structure

The transverse section of *M. tuberosa* leaf blade from the outermost to the internal layer was composed of adaxial and abaxial epidermal tissue covered by cuticle; hypodermis under the adaxial epidermis, palisade, spongy mesophyll, and vascular bundles (Figure 2a).

The adaxial and abaxial epidermal cells have a polygonal shape with straight indented cell walls (Figures 2b and 2c). The hypodermal tissue comprises two layers of cells, larger than the epidermal cells. The tissues serve to reduce water loss during transpiration. Palisade tissue consisted of two layers of cells extending vertically in a tight arrangement. Spongy mesophyll tissue was composed of various and irregular-shaped cells. Stomata were found only on the abaxial leaf blade (hypostomatic) (Figure 2c). The location of stomata helps reduce water loss excess (Martin and Glover 2007; de Souza Lima et al. 2020). *M. tuberosa* has parasitic-type stomata, with two or more accessory cells parallel to the guard cells (Cotthem 1970). Parasitic-type stomata were also found in *Mitracarpus hirtus*, *Mussaenda chippii*, and many others belonging to the Rubiaceae family (Obembe 2015). Apart from the parasitic type, anomocytic and anisocytic stomata were also found in this family (Patil and Patil 2011; Obembe 2015). *M. tuberosa* petiole comprises a cuticle layer, epidermis, cortex, cortex containing chloroplast (chlorenchyma), and vascular bundles (Figure 2d).

The tissues that made up the domatium from the outermost to the internal layer consisted of the periderm, cortex, vascular bundles, and pith (Figure 2e). The pith network consisted of polygonal-shaped cells, which were

smaller in size than the cortical cells (Figure 2e). The periderm was composed of phellem tissue, *i.e*., dead cells that function as a substitute for epidermal tissue. Phellogen tissue was located inside the phellem tissue, consisting of one or several layers of rectangular cells, while the phelloderm was situated below the phellogen tissue. Phelloderm cells resembled in shape with polygonal cortical cells (Figure 2f). The same thing was observed in the outermost layer of *M. pendens* domatium, which was dominated by phellem cells and produced true spines, which protected the plant from herbivores and excessive water loss (Huxley 1978). The vascular bundles in the domatium consisted of a thick-walled xylem and a thin-walled phloem (Figure 2g).

Histochemistry and secretory structure

The histochemical tests of *M. tuberosa* showed the accumulation of phenolic compounds scattered over various tissues, *i.e.*, the leaf blade, petiole, and domatium. Specific methods, including the histochemical methodology, are needed to study secretory structures and the presence of secondary metabolites in plants. Histochemistry is a branch of histology that investigates the location of secondary metabolite accumulation in various secretory structures and tissues by qualitatively staining as a specific indicator (Demarco 2017). The presence of phenolics was indicated by the formation of a black-green color in the reaction with ferric chloride ($FeCl_3$). Figures 3a-c show the control of the leaf blade, petiole, and domatium without reagent. Phenolic compounds in the leaf blade were accumulated in idioblast, scattered over the palisade tissue, spongy tissue, and intercellular spaces (Figure 3d).

Petiole accumulated phenolic compounds in the epidermis, idioblasts scattering over the cortex, intercellular spaces of the cortex, and chlorenchyma cells (Figure 3e). In comparison, domatium accumulated phenolic compounds in idioblasts of the periderm, cortex, pith, and the intercellular spaces of the cortex and pith (Figure 3f). Phenolics are potential antioxidant~~s~~ against free radicals (Haq et al. 2011; Nardini 2022). Phenolic compounds are secondary metabolites in a plant's most significant quantities. They have various antioxidant activities through different mechanisms, such as reducing agents, free radical scavengers, metal chelating, and electron donors (Camargo et al. 2016). *M. pendens* was reported to contain components with certain antioxidant activity, attributed to the phenol group (Dhurhania and Novianto 2018).

Identification of flavonoid compounds using aluminum chloride reagent ($AlCl_3$) showed positive results on the leaf blade, petiole, and domatium of *M. tuberosa*. The formation of blue fluorescence indicated a positive reaction. The accumulated flavonoids may be of the flavonols type because they produced a blue glow when observed under a fluorescence microscope. Guerin et al. (1971) identified the presence of three kinds of flavonoids, namely flavones (greenish-yellow), flavanones (yellow), and flavonols (blue). Flavonoids were identified in the spongy tissues and hypodermis of the leaf blade (Figure 4a), whereas in the petiole, only idioblasts in the cortex contained flavonoids (Figure 4b).

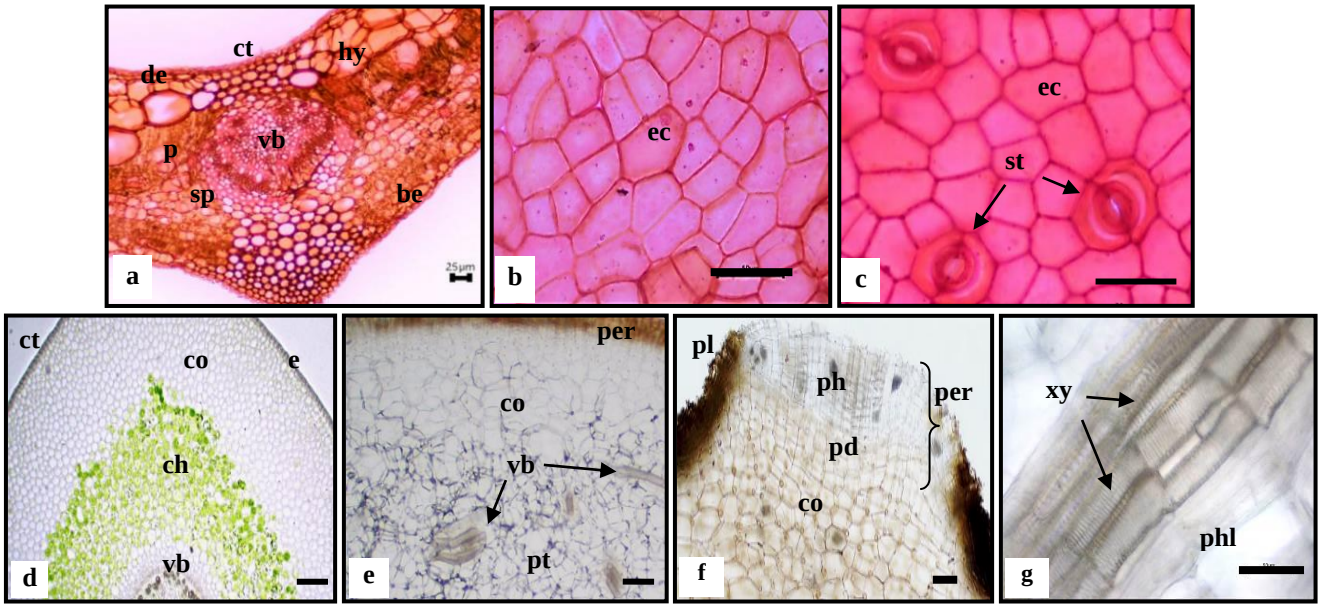

Figure 2. Transverse and paradermal sections of leaf blade, petiole, and domatium of *Myrmecodia tuberosa*. (a) anatomy of leaf blade, (b) paradermal section of the adaxial epidermis of the leaf blade, (c) paradermal section of the abaxial epidermis of the leaf blade, (d) anatomy of petiole, (e, f, g) anatomy of domatium. Cuticle (ct), adaxial epidermis (de), hypodermis (hy), palisade (p), spongy mesophyll (sp), vascular bundles (vb), abaxial epidermis (be), epidermis cells (ec), stomata (st), cortex (co), chlorenchyma (ch), periderm (per), pith (pt), phellem (pl), phellogen (ph), phelloderm (pd), phloem (phl), xylem (xy). Bar scale 25 µm (a), 50 µm (b- g)

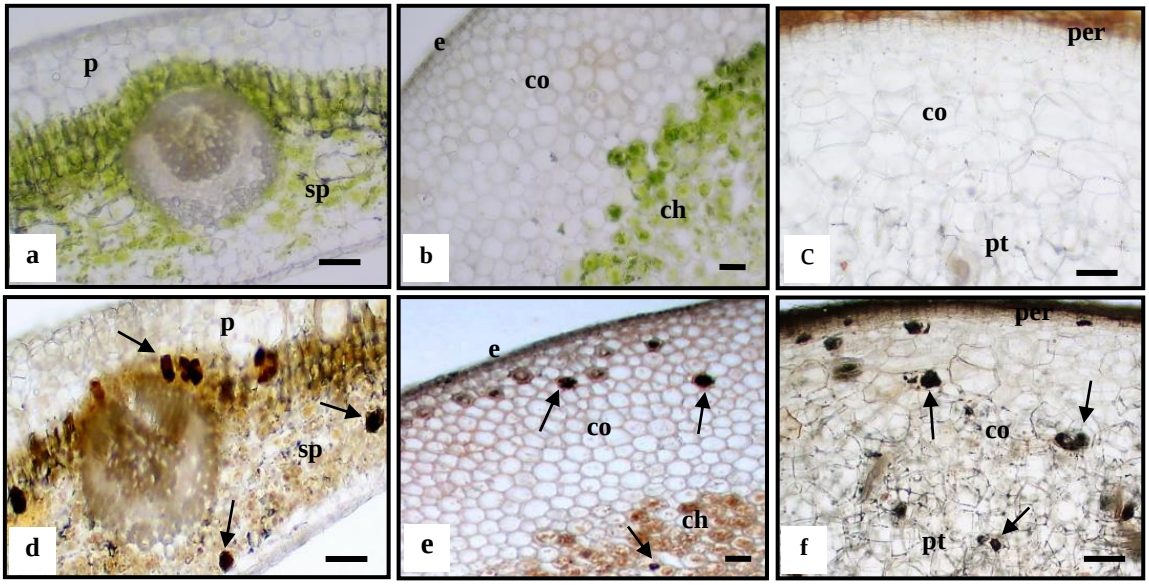

Figure 3. Ferric chloride test for phenolics in leaf blade, petiole, and domatium of *Myrmecodia tuberosa*, marked by greenish-dark brown color. (a) Leaf blade control, (b) petiole control, (c) domatium control, (d) phenols in idioblast among the palisade, spongy tissue, and intercellular spaces of the leaf blade, (e) accumulation in petiole tissue and idioblasts, (f) accumulation in domatium tissue and idioblasts. Black arrows = phenol-accumulating idioblasts, epidermis (e), palisade (p), spongy tissue (sp), cortex (co), chlorenchyma (ch), pith (pt), periderm (per). Scale bar 25 µm (b,e), 50 µm (a,c,d, and d)

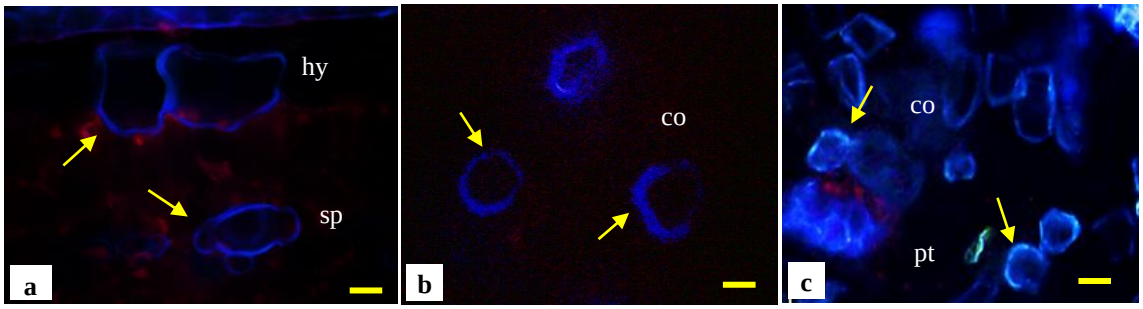

Figure 4. Flavonoids in the leaf blade, petiole, and domatium of *Myrmecodia tuberosa*. (a) accumulation of flavonoids in the idioblast of spongy tissues and hypodermis of the leaf blade, (b) in idioblast of the petiole cortex, (c) in idioblast of the cortex, and pith of domatium. Yellow arrows: idioblast cells; hypodermis (hy), spongy (sp), cortex (co), pith (pt). Scale bar 50 µm

Flavonoids were found also in the domatium, distributed over the cortex and pith (Figure 4c). Domatium seemed to accumulate more flavonoids than the leaf blade and petiole; therefore, *M. tuberosa* domatium is widely used as an alternative medicine for cancer and tumors. The ethanol extract of domatium of this species was reported to reduce tumor growth and induce apoptosis of oral carcinoma cells (Yuletnawati et al. 2016) and had a cytotoxic effect on MCF-7, HT-29 and HELA cells (Rasemi et al. 2014). In addition, the domatium was potentially antidiabetic (Raya et al. 2016). Those medicinal effects might be attributed to the flavonoid flavonols contained in the domatium.

Flavonols are abundant in various fruits, vegetables, tea, and red wine (Panche et al. 2016). The most studied flavonols are kaempferol, quercetin, myricetin, and fisetin, which are considered to have potential against bladder and prostate cancers (Crocetto et al. 2021), head and neck cancers (Kubina et al. 2021) or gastric adenocarcinoma (Wang et al. 2022).

Histochemical assays using 5% copper acetate indicated the presence of terpenoid compounds, marked by reddish-brown or brownish-yellow color in the tissue. The terpenoid test controls on the leaf blade, petiole, and domatium tissues are shown in Figures 5a, b, and c, respectively. These compounds were accumulated in idioblasts of the leaf blade, situated among the palisade and spongy tissue (Figure 5d). In the petiole, terpenoids were only identified in idioblasts among the cortex cells (Figure 5e). In contrast, terpenoids were distributed to almost all tissues in the domatium, i.e., idioblasts, periderm, cortex, and pith (Figure 5f). Terpenoids are the second most abundant compounds of natural products, a group of important secondary metabolites in plants. They have

several direct and indirect defensive functions against herbivores and abiotic stresses and serve as signaling molecules (Kromer et al. 2016), play an important role in plant growth and development, physiological processes, and in the interaction between plants and the environment in form of phytoalexins and as interspecific sensing compounds (Arimura et al. 2000). Terpene compounds also have pharmacological effects as anticancer and anti-inflammatory, and serve as integral component of vitamins, such as A, E, and K (Sankhla et al. 2022; Ratnadewi et al. 2023).

The existence of essential oils was marked by the formation of blue color after reacting with the NADI reagent. Controls on the leaf blade, petiole, and domatium are shown in Figures 6a, b, and c, respectively. Essential oils were identified in idioblasts among the palisade and spongy tissues and accumulated in the leaf blade cuticle (Figure 6d). Essential oils in the petiole accumulated in the cuticle layer, epidermal tissue, and idioblasts distributing in the cortex and chlorenchyma tissue (Figure 6e). Essential oils were detected in idioblast cells of the cortex, pith, and the domatium's periderm (Picture 6f).

Essential oils are concentrated liquids of complex mixtures of aromatic hydrophobic oily volatile compounds. They can be extracted from different plant parts, such as bark, buds, flowers, fruits, leaves, peels, roots, seeds, twigs, or the whole plant~~s~~ of a single botanical source. Structurally, the chemical constituents of essential oils can be classified into four groups: terpenes, terpenoids, phenylpropanoids, and other components (Hyldgaard et al. 2012)

Identification of lipophilic compounds by Sudan IV reagent showed positive results, indicated by the orange color in the tissue and secretory structures. Lipophilic test controls on leaf blade tissue, petiole, and domatium are shown in Figures 7a, b, and c, respectively.

Lipophilic compounds in the leaf blade were accumulated in idioblasts, palisade, spongy tissue, and cuticle layer (Figure 7d). In the petiole, these compounds were detected in the cuticle layer and idioblasts in the epidermis and cortex (Figure 7e). Lipophilic compounds in domatium accumulated in the intercellular spaces of the periderm tissue and within the idioblasts of the cortical area (Figure 7f).

The identification of alkaloids was carried out by using a Wagner reagent. Figure 8a is the negative control for alkaloids. The alkaloids test showed positive results in the epidermis, idioblasts in chlorenchyma, and vascular bundles of the petiole (Figure 8b). A test carried out by tartaric acid, showing negative in alkaloids, is presented in Figure 8c. Alkaloids in leaf blade and domatium were not detected, although a phytochemical test by Demetillo et al. (2017) showed that *M. tuberosa* domatium contained alkaloid compounds. It might happen because the leaf blade and domatium's alkaloids were measly, and could not be detected by the histochemical test.

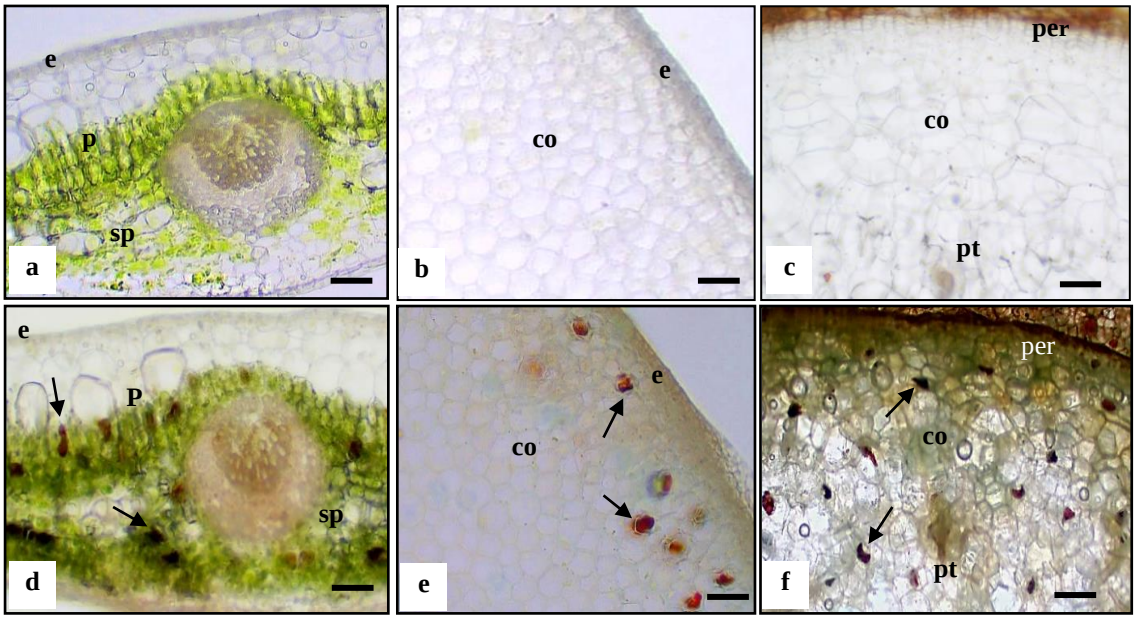

Figure 5. Terpenoid content in the leaf blade, petiole, and domatium of *Myrmecodia tuberosa* was revealed by 5 % copper acetate. (a) leaf blade control, (b) petiole control, (c) domatium control, (d) terpenoids in idioblast among the palisade and spongy tissue of leaf blade, (e) idioblasts in the cortex of petiole, (f) idioblasts, periderm, cortex, and pith of domatium. Black arrows = idioblast cells accumulating terpenoids, epidermis (e), palisade (p), spongy (sp), cortex (co), periderm (per), and pith (pt). Scale bar 50 µm

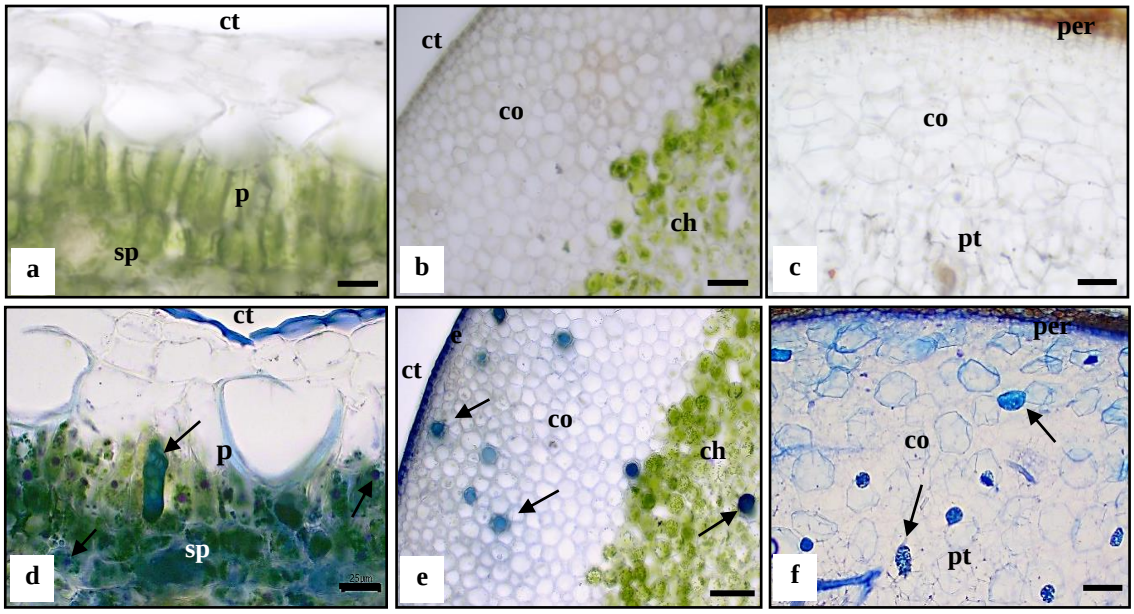

Figure 6. Essential oils in the leaf blade, petiole, and domatium of *Myrmecodia tuberosa* were detected with NADI reagent. (a) Leaf blade control, (b) petiole control, (c) domatium control, (d) essential oils in idioblasts in palisade, spongy tissue areas, and in the cuticle of leaf blade, (e) essential oil in idioblasts in cortex, epidermis, chlorenchyma and cuticle of petiole, (f) in idioblasts of cortex, pith and periderm of domatium. Black arrow = idioblasts. Cuticle (ct), epidermis (e), palisade (p), spongy (sp), cortex (co), chlorenchyma (ch), pith (pt), and periderm (per). Scale bar 50µm (b, c, e, and f), 25 µm (a and b)

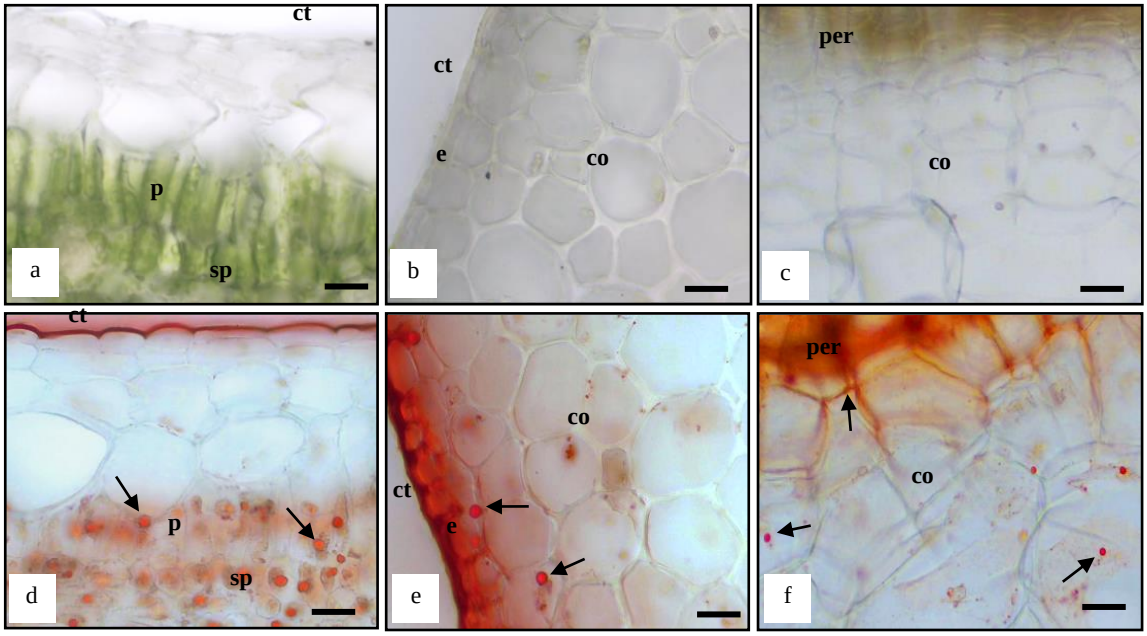

Figure 7. Lipophilic content in leaf blade, petiole, and domatium of *Myrmecodia tuberosa*. (a) leaf blade control, (b) petiole control, (c) domatium control, (d) accumulation of lipophilic in idioblasts, palisade, and spongy tissue, and cuticle of the leaf blade, (e) in cuticle, epidermis, idioblasts and cortex of the petiole, (f) in domatium periderm, cortex, and idioblasts. Black arrows = idioblast cells. Cuticle (ct), epidermis (e), palisade (p), spongy (sp), cortex (co), periderm (per). Scale bar 25 µm

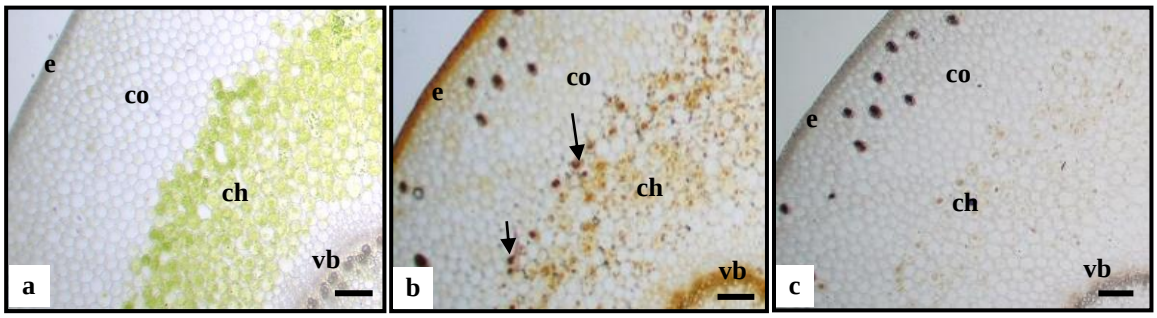

Figure 8. Alkaloids are found in epidermis, chlorenchyma, vascular bundles cells, and idioblasts of *Myrmecodia tuberosa* petiole. (a) Alkaloid test control with aquadest, (b) alkaloid revealed by Wagner reagent, (c) negative control of alkaloids with tartaric acid. Black arrows = idioblast cells; epidermis (e), cortex (co), chlorenchyma (ch), and vascular bundles (vb). Scale bar 50 µm

The results of histochemical analysis on the leaf blade, petiole, and domatium ensured that the three organs contained secondary metabolites. Secondary metabolites of *M. tuberosa* were detected in the common spaces, such as cuticle and intercellular spaces, and the secretory structures were dominated by idioblasts (Table 1). Idioblasts can be observed by using specific reagents. This is due to its form, which is similar to that of surrounding cells, and it can only be distinguished from its compounds by specific reagents (Kuster and Vale 2016).

Secondary metabolites produced by plants are important in defense against parasites, herbivores, and fungi (Khare et al. 2020). Besides providing benefits to the producing plant, humans utilize specific secondary metabolites as raw materials for medicinal ingredients because of their diverse pharmacological effects. Histochemical tests performed on the leaf, petiole, and domatium of *M. tuberosa* unveiled that this plant contained phenolics, flavonoids, terpenoids, essential oils, and lipophilics. In contrast, alkaloids were only found in the petiole. Phenolics were the most accumulated compounds among other secondary metabolites in this species. *M. tuberosa* has a lot of benefits, among others, as an alternative medicine to treat cancers. This was due to the content of phenolics and flavonoids' ability to scavenge free radicals (Othman et al. 2014). Hasanuddin et al. (2015) reported that terpenoid compounds isolated from *M. pendens* could reduce cell growth and induce ovarian cancer cell apoptosis (SKO-3). Meanwhile, *M. tuberosa* has the potential as an antimicrobe that inhibits the growth of *Candida albicans*, *Escherichia coli*, and *Staphylococcus aureus* (Effendi and Hertiani 2013).

Table 1. Distribution of secondary metabolites and idioblast cells in various tissues of the leaf blade, petioles, and domatium *of Myrmecodia tuberosa*

Organs	Location	Secretory structure	Histochemical tests for					
			Phenols	Flavonoids	Terpenoids	Essential oils	Lipophilic	Alkaloids
Leaf blade	Cuticle	-	-	-	-	+	+	-
	Epidermis	Idioblast	-	-	-	-	-	-
	Hypodermis	Idioblast	-	-	-	-	-	-
	Palisade	Idioblast	+	-	+	+	+	-
	Spongy mesophyll	Idioblast	+	+	+	+	+	-
	Intercellular spaces	-	+	-	-	-	-	-
Petiole	Cuticle	-	-	-	-	+	+	-
	Epidermis	-	+	-	-	+	-	+
	Epidermis	Idioblast	-	-	-	-	+	-
	Cortex	Idioblast	+	+	+	+	+	-
	Chlorenchyma	Idioblast	+	-	-	+	-	+
	Vascular bundles	-	-	-	-	-	-	+
	Intercellular spaces	-	+	-	-	-	-	-
Domatium	Periderm	Idioblast	+	-	+	+	-	-
	Cortex	Idioblast	+	+	+	+	+	-
	Pith	Idioblast	+	+	+	+	-	-
	Intercellular spaces	-	+	-	-	-	+	-

Note: + (compound detected), - (no compound detected)

FTIR spectra and functional groups

The FTIR spectra of the leaf blade and petiole of *M. tuberosa* show the same pattern, while the spectra of domatium demonstrated a slightly different pattern in the fingerprint region (Figure 9). It indicates that the metabolites found in the leaf blade and petiole are similar, while domatium slightly varies in metabolites content. For example, the difference in peak intensity occurred at wave numbers 3398 cm^{-1} in domatium and 3397 cm^{-1} in leaf blade and petiole, which was the stretching vibration of the hydroxyl (−OH) functional group. Fourier Transform Infrared (FTIR) is an instrument used to determine the vibrational spectrum of molecules to predict the chemical structure based on the identified functional groups (Sulistyani 2018). Qualitative parameters in FTIR can be observed from the wave numbers that arise due to absorption by a functional group, typical of a compound. According to Purwakusumah et al. (2014), band positions and intensities in an FTIR spectrum correlate with the changes in its chemical composition. The generated FTIR fingerprint spectrum is very complex data information, so the results thoroughly describe the chemical characteristics of a sample.

The absorbance of the -OH group in the domatium was more significant than those in the other organs, which can be seen from the peaks produced. It may be the reason for *M. tuberosa* domatium to have more excellent antioxidant activity than the leaf blade and petiole. Antioxidant activity can be influenced by metabolites, such as phenolic and flavonoid groups, which contain many hydroxyl and methyl groups.

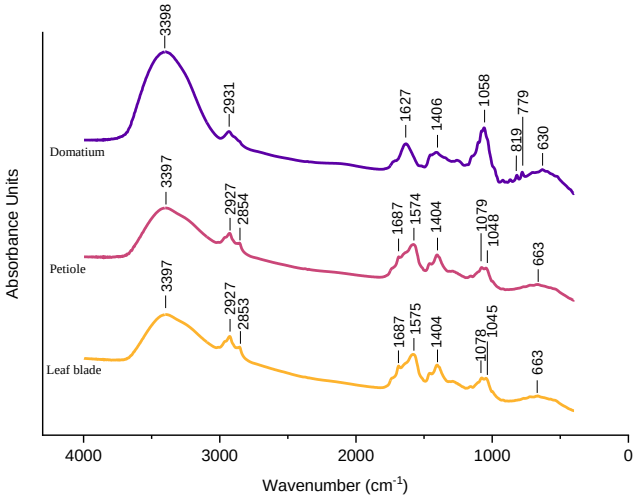

Figure 9. FTIR spectra of leaf blade, petiole, and domatium extracts of *Myrmecodia tuberosa*

In general, the functional groups contained in the three types of organs were almost the same, including the functional groups -OH (alcohols, phenols, and carboxylic acids), -CH (alkane, aromatics), -CO (alcohols and ethers), NH (secondary amine), CX (chloride and bromide). The wave numbers of each functional group are summarized in Table 2. The functional group contained only the leaf blade and the petiole was NH (secondary amine). The functional groups -CH (aromatic) and CX (bromide, iodide) were present only in the domatium.

Table 2. Identification of the functional groups of the compounds detected in the leaf blade, petiole, and domatium of *Myrmecodia tuberosa*

Sample	Sample wavenumber (cm^{-1})	Reference* wavenumber (cm^{-1})	Functional group
Leaf blade	3397	3570-3200	–OH stretch (Alcohol and hydroxy compound)
	2927	3000-2840	C–H (Alkane)
	2853	3000-2840	C–H (Alkane)
	1687	1640-1550	N–H bend (Secondary amine)
	1575	1640-1550	N–H bend (Secondary amine)
	1404	1410-1310	–OH (Phenol)
	1078	1300-1000	–CO stretch (Primary alcohol)
	1045	1070-1027	–CO stretch (Ether)
	663	705-570	C–X (Chloride)
Petiole	3397	3570-3200	−OH stretch (Alcohol and hydroxy compound)
	2927	3000-2840	C–H (Alkane)
	2854	3000-2840	C–H (Alkane)
	1687	1640-1550	N–H bend (Secondary amine)
	1574	1640-1550	N–H bend (Secondary amine)
	1404	1410-1310	–OH (Phenol)
	1079	1300-1000	–CO stretch (Primary alcohol)
	1048	1070-1027	–CO stretch (Ether)
	663	705-570	C–X (Chloride)
Domatium	3398	3570-3200	–OH stretch (Alcohol and hydroxy compound)
	2931	3000-2840	C–H (Alkane)
	1627	1680-1620	C=C stretch (Alkene)
	1406	1410-1310	–OH (Phenol)
	1058	1070-1027	–CO stretch (Ether)
	819	860-800	C–H (Aromatics)
	779	785-540	C–X (Chloride)
	630	630	C–X (Bromide, iodide)

Note: *Coates 2000; Pavia 2015; Nandiyanto et al. 2019

Grouping of leaf blade, petiole, and domatium metabolites by PCA

PCA helped to classify *M. tuberosa* extracts based on different plant organs with FTIR data. The spectral pattern, which was almost the same for the three samples, made it difficult to distinguish using only the FTIR spectrum. Therefore, chemometric methods were needed in this case. The grouping of leaf blades, petiole, and domatium can be presented in a two-dimensional score plot (Figure 10). This PCA plot shows the patterns in the IR spectrum; the closer one point is to another, the greater the similarity between the IR spectra of the samples, so that we can see the similarities and differences in the functional groups between samples. Based on the PCA results, the organ samples can be appropriately classified because the samples are already clustered. The leaf blade and petiole have groups that are close together, which indicates that the metabolite components in the leaf blade and petiole have similar contents. In contrast, the domatium has groups quite far apart, showing more significant differences in metabolites contents with the other two plant organs.

The principal component (PC) is a score plot, a projection of several objects. The score plot shows that the closer one sample is to another, the greater the similarity between the samples' metabolite profiles (Purwakusumah et al. 2014). The score plot for the first two PCs is usually the most useful in the analysis because these two PCs contain the most variation in the data. The wavelength used for PCA analysis ranges from 4000-400 cm^{-1}. PCA can make it easier to visualize data groupings, evaluate similarities between groups or classes, and find factors or reasons behind the observed patterns through correlations based on the chemical or physical properties of the sample (Rafi et al. 2016). The PC exhibited 98% (PC-1, 82.1% and PC-2, 15.9%) of the explained variance when the FTIR spectrum data were analyzed using PCA. The cumulative percentage of PC-1 and PC-2 from the two data has to be more than 70% to visualize the plot score well in two dimensions (Esteki et al. 2018).

The research on *M. tuberosa* concludes that this species has a hypostomatic leaf blade with parasitic stomata. The main secretory structure was idioblast. Idioblasts were scattered in various tissues, such as the epidermis, hypodermis, palisade, spongy mesophyll, and cuticle of the leaf blade, in the epidermal tissue, chlorenchyma cortex, and cuticle of the petiole. They were distributed in the domatium's periderm, cortex, and pith. Terpenoids, phenols, lipophilic compounds, essential oils, and flavonoids were present in the leaf blade, petioles, and domatium, whereas alkaloids were found only in the petiole. The FTIR spectra of the leaf blade and petiole showed quite similar patterns. In contrast, the spectra of domatium showed a slightly different pattern from the two others in the fingerprint region. It is indicated that the secondary metabolites found in the leaf blade and petiole are almost identical, while domatium has a slightly different metabolites content. The -NH (secondary amine) functional group was present only in the leaf blade and petiole, while the -CH (aromatic) and -CX (bromide, iodide) functional groups were found only in the domatium.

Antioxidant activities

The antioxidant activities of the leaf, petiole, and domatium are represented by the IC_{50} values (Table 3). It demonstrates that domatium has the highest capacity in inhibiting oxidation due to free radicals, compared to the two other organ tissues. The lower the IC_{50} value, the more powerful its antioxidant activity is. Domatium is richer in secondary metabolites content, particularly in phenolics and flavonoids, as detected by the histochemical tests. Secondary metabolites, such as phenolics, flavonoids, and terpenoids in *M. tuberosa*, showed antioxidant activities (Sari et al. 2017). DPPH serves as a free radical that reacts with a sample through a hydrogen-atom transfer mechanism or the single electron transfer, depending on the antioxidants, free radicals, and the reaction environment. (Baschieri and Amorati 2021).

Figure 11 presents the result of PLS-DA correlating the functional groups and the IC_{50} values of leaf blade, petiole, and domatium. Of the 18 functional groups identified in this study, 13 significantly correlate with its antioxidant activity. The horizontal bars in the negative area indicate the correlation with antioxidant activity, while the bars in the positive area relate to a less active antioxidant (Focker et al. 2021). This is in line with the low value of IC_{50}, which means it has a high scavenging capacity. The OH, C–O, C–X, and aromatic C–H groups contribute to the antioxidant activities. The groups attached to some secondary metabolites were known to have the capacity to neutralize free radicals, including ROS, to chelate to form pro-oxidant species and to stimulate the activity of intracellular antioxidant enzymes (Ratnadewi et al. 2023).

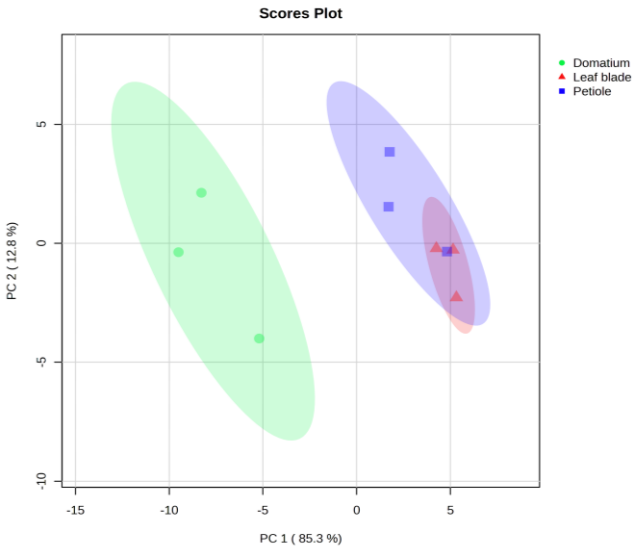

Figure 10. Plot of PCA scores for leaf blade (▲), petiole (■), and domatium (●) metabolites of *Myrmecodia tuberosa*

Table 3. Values of antioxidant activity of sample extracts of leaf blade, petiole, and domatium of *M. tuberosa* through DPPH method

Sample	Antioxidant activity (IC_{50} in µg/mL*)
Ascorbic acid	2,68±0,90[c]
Leaf blade	423,96±7,32[a]
Petiole	418,68±2,41[a]
Domatium	150,83±1,67[b]

Note: *) means of 3 replicates and standard deviation. Samples followed by the same alphabet are not significantly different by DMRT test at α=5%

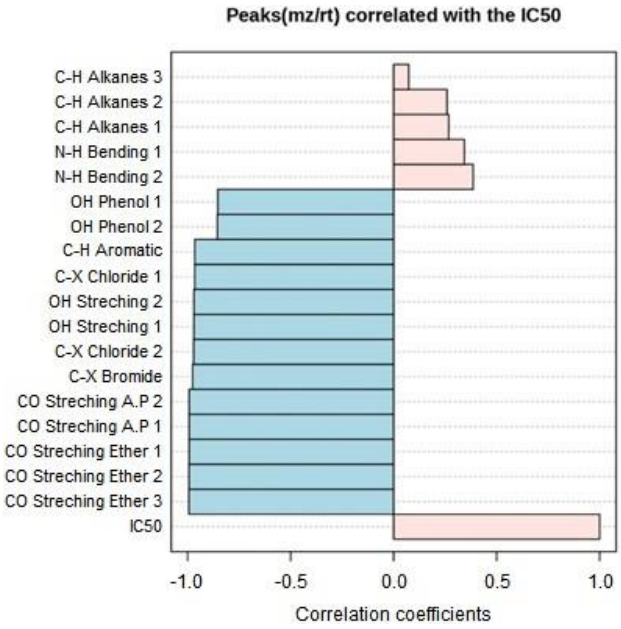

Figure 11. The correlation between the antioxidant activity (IC_{50}) and the functional groups identified in the leaf blade, petiole, and domatium of *M. tuberosa*

REFERENCES

Arimura G, Ozawa R, Shimoda T, Nishioka T, Boland W, Takabayashi J. 2000. Herbivory-induced volatiles elicit defence genes in lima bean leaves. Nature 406 (6795): 512-515. DOI: 10. 1038/35020072.

Baschieri A, Amorati R. 2021. Methods to determine chain-breaking antioxidant activity of nanomaterials beyond DPPH: A review. Antioxidants 10: 1551. DOI: 10.3390/antiox10101551.

Boix YF, Victório CP, Defaveri ACA, do Carmo de Oliveira Arruda R, Sato A, Lage CLS. 2011. Glandular trichomes of *Rosmarinus officinalis* l: Anatomical and phytochemicalsanalyzes of leaf volatiles. Plant Biosyst 145 (4): 848-856. DOI: 10.1080/11263504.2011.584075.

Cahyaningsih R, Brehm JM, Maxted N. 2021. Setting the priority medicinal plants for conservation in Indonesia. Genet Resour Crop Evol 68: 2019-2050. DOI: 10.1007/s10722-021-01115-6.

Camargo JM, Dunoyer AT, Garcia-Zapateiro LA. 2016. The effect of storage temperature and time on total phenolics and enzymatic activity of sapodilla (*Achras sapota* L.). Revista Facultad Nacional de Agronomía Medellín 69 (2): 7955- 7963. DOI: 10.15446/rfna.v69n2.59140.

CHAH (Council of Heads of Australasian Herbaria). 2011. Australian Plant Census. https://biodiversity.org.au/nsl/services/rest/node/apni/2903039.

Coates J. 2000. Interpretation of infrared spectra, a practical approach. EAC 12: 10815-10837. DOI: 10.1002/9780470027318.a5606.

Coelho dM, Leite JPV, Fietto LG, Ventrella MC. 2013. Colleters in *Bathysa cuspidata* (Rubiaceae): development, ultrastructure and chemical composition of the secretion. Flora-Morphol Distrib Funct Ecol Plants 208 (10-12): 579-590. DOI: 10.1016/j.flora.2012.08.005.

Crocetto F, Erika Z, Carlo B, Achille A, Savio DP, Biagio B, Francesco T, Vincenzo FC, Luca S, Matteo F, et al. 2021. Kaempferol, myricetin and fisetin in prostate and bladder cancer: a systematic review of the literature. Nutrients 13 (11): 3750. DOI: 10.3390/nu13113750.

David R, Carde JP. 1964. Histochimie-coloration differentielle des inclusions lipidiques et terpeniques des pseudophylles du pin maritime au moyen du reactif NADI. Comptes Rendus Hebdomadaires Des Seances De L Academie Des Sciences 258 (4): 1338.

de Souza Lima MP, Soares A, Porto JMP, Sá FS, Carvalho MS, Braga FT. 2020. Leaf anatomy of Rubiaceae species in a semiarid area of Brazil. Rodriguésia 70: e01562018. DOI: 10.1590/2175-7860202071096.

Demarco D. 2017. Histochemicals analysis of plant secretory structures. In: Pellicciari C, Biggiogera M (eds). Histochemistry of Single Molecules. Methods in Molecular Biology. Springer, New York. DOI: 10.1007/978-1-4939-6788-9_24.

Demetillo M, Uy M, Baguio M, Nuneza O. 2017. Phytochemical analysis and cytotoxic activity of ant plant (*Myrmecodia tuberosa* Jack.). JBES 11 (6): 85-91.

Dhurhania CE, Novianto A. 2018. Test of total phenolic content and its effect on antioxidant activity of various dosage forms ant-plant (*Myrmecodia pendens*). Jurnal Ilmu Kefarmasian Indonesia 5 (2): 62-68. DOI: 10.20473/jfiki.v5i22018.62-68.

Efendi YN, Hertiani Q. 2013. Antimicrobial potency of ant-plant extract (*Myrmecodia tuberosa* Jack.) against *Candida albicans*, *Escherichia coli*, and *Staphylococcus aureus*. Tradit Med J 18 (1): 53-58. DOI: 10.22146/tradmedj.7944.

Esteki M, Simal-Gandara J, Shahsavari Z, Zandbaaf S, Dashtaki E, Vander Heyden Y. 2018. A review on the application of chromatographic methods, coupled to chemometrics, for food authentication. Food Control 93: 165-182. DOI: 10.1016/J.FOODCONT.2018.06.015.

Focker M, Cecil A, Prehn C, Adamski J, Albrecht M, Adams F, Hinney A, Libuda, L, Bu¨hlmeier J, Hebebrand J, Peters T, Antel J. 2021. Evaluation of metabolic profiles of patients with anorexia nervosa at inpatient admission, short- and long-term weight regain—descriptive and pattern analysis. Metabolite 11 (1): 7. DOI: org/10.3390/ metabo11010007.

Furr M, Mahlberg PG. 1981. Histochemical analyzes of laticifers and glandular trichomes in *Cannabis sativa*. J Nat Prod 44 (2): 153-159. DOI: 10.1021/np50014a002.

Greenfield MJ, Lach L, Congdon BC, Anslan S, Tederso L, Field M, Abell SE. 2021. Consistent patterns of fungal communities within ant-plants across a large geographic area range strongly suggest a multipartite mutualism. Mycol Prog 20: 681-699. DOI: 10.1007/s11557-021-01690-z.

Guerin HP, Delaveau PG, Paris RR. 1971. Localizations histochimiques: II: Procédés simplesde localization de pigments flavoniques. Application a quelques phanérogames. Bulletin de la Société botanique de France 118 (12): 29-36. DOI: 10.1080/00378941.1971.10838874.

Haq M, Sani W, Hossain ABMS, Taha RM, Monneruzzaman KM. 2011. Total phenolic contents, antioxidant and antimicrobial activities of *Bruguiera gymnorrhiza.* J Med Plants Res 5 (17): 4112-4118.

Hasanuddin, Rifayani KF, Supriadi G, Kurnia D, Adhita D. 2015. Potential of terpenoids bioactive compound isolated from Papua ant-plant as an alternative to ovarian cancer treatments. Open J Obstet Gynecol 5: 406-411. DOI: 10.4236/OJOG.2015.57058.

Huxley CR, Jebb MHP. 1993. The tuberous Epiphytes of the Rubiaceae 5: a revision of *Myrmecodia*. Blumea 37: 271-334.

Huxley CR. 1978. The ant-plants *Myrmecodia* and *Hydnophytum* (Rubiaceae), and the relationships between their morphology and occupants, physiology and ecology. New Phytol 80: 231-268. DOI: 10.1111/j.1469-8137.1978.tb02285.x.

Hyldgaard M, Mygind T, Meyer RL. 2012. Essential oils in food preservation: Mode of action, synergies, and interactions with food matrix components. Front Microbiol 3: 1-24. DOI: 10.3389/fmicb.2012.00012.

Indra P, Supriadi, Ijirana. 2019. Test of the antioxidant activity of ant-plant (*Myrmecodia tuberosa* Jeck) extract from Tolitoli District, Central Sulawesi. Jurnal Akademika Kimia 8 (2): 98-103. DOI: 10.22487/j24775185.2019.v8.i2.2754. [Indonesian]

Johansen DA. 1940. Plant Microtechnique. McGraw-Hill, New York.

Khare S, Singh NB, Singh A, Hussain I, Niharika K, Yadav V, Bano C, Yadav RK, Amist N. 2020. Plant secondary metabolites synthesis and

their regulations under biotic and abiotic constraints. J Biol 63 (3): 203-216. DOI:10.1007/s12374-020-09245-7.
Kromer K, Kreitschitz A, Kleinteich T, Gorb SN, Szumny A. 2016. Oil secretory system in vegetative organs of three Arnica taxa: Essential oil synthesis, distribution and accumulation. Plant Cell Physiol 57 (5): 1020-1037. DOI: 10.1093/pcp/pcw040.
Kubina R, Iriti M, Kabała-Dzik A. 2021. Anticancer potential of selected flavonols: Fisetin, kaempferol, and quercetin on head and neck cancers. Nutrients 13*:* 845. DOI: 10.3390/nu13030845.
Kuster VC, Vale F. 2016. Leaf histochemistry analysis of four medicinal species from Cerrado. Braz J Pharm Sci 26 (6): 673-678. DOI: 10.1016/j.bjp.2016.05.015.
Lange BM. 2015. The evolution of plant secretory structures and emergence of terpenoids chemical diversity. Annu Rev Plant Biol 66: 139-159. DOI: 10.1146/annurev-arplant-043014-114639.
Mardany MP, Chrystomo LY, Karim AK. 2016. Screening phytochemicals and test activity cytotoxic from ant-plant (*Myrmecodia beccarii* Hook.f.) from the District Merauke. Jurnal Biologi Papua 8 (1): 13-22. DOI: 10.31957/jbp.41. [Indonesian]
Martin D, Tholl D, Gershenzon J, Bohlmann J. 2002. Methyl jasmonate induces traumatic resin ducts, terpenoid resin biosynthesis, and terpenoid accumulation in developing xylem of Norwegian spruce stems. Plant Physiol 129 (3): 1003-1018. DOI: 10.1104/pp.011001.
Martin C, Glover BJ. 2007. Functional aspects of cell patterning in aerial epidermis. Curr Opin Plant Biol 10 (1): 70-82. DOI: 10.1016/j.pbi.2006.11.004.
Nandiyanto ABD, Oktiani R, Ragadhita R. 2019. How to read and interpret ftir spectroscope of organic material. J Sci Technol 4 (1): 97-118. DOI: 10.17509/ijost.v4i1.15806.
Nardini M. 2022. Phenolic compounds in food: characterization and health benefits. Molecules 27 (3): 783. DOI: 10.3390/molecules27030783.
Nurhasanah, Iriani D. 2021. Histochemical test of root, petiole and leaf of Kelembak (*Rheum officinale* Baill.). Jurnal Biologi Tropis 21 (3): 726-733. DOI: 10.29303/jbt.v21i3.2858. [Indonesian]
Obembe OA. 2015. Studies on the stomata of some Rubiaceae. Acad Res Intern 6 (4): 17-23. www.journals.savap.org.pk.
Othman A, Mukhtar NJ, Ismail NS, Chang SK. 2014. Phenolics, flavonoids content and antioxidant activities of 4 Malaysian herbal plants. Intl Food Res J 21 (2): 759.
Panche AN, Diwan AD, Chandra SR. 2016. Flavonoids: an overview. J Nutr Sci 5 (57): 1-15. DOI: 10.1017/jns.2016.41.
Patil CR, Patil DA. 2011. Investigations on foliar epidermis in some Rubiaceae. J Phytol 3 (12): 35-40.
Pavia DL, Lampman GZ, Kriz GZ. 2015. Introduction to Spectroscopy. Thompson Learning Inc., Washington (US).
Purwakusumah ED, Rafi M, Syahfitri UD, Nurcholis W, Adzkiya MAZ. 2014. Identification and authentication of red ginger using a combination of FTIR spectroscopy and chemometrics. Agritech 34 (1): 82-87. DOI: 10.22146/agritech.9526.
Rafi M, Anggundari WC, Irrawaddy TT. 2016. Potential of Ftir-Atr spectroscopy and chemometrics to distinguish hair from pigs, goats and cattle. Indonesia. J Chem Sci 5 (3): 229-234. DOI: 10.15294/IJCS.V5I3.10654.
Rafi M, Rismayani W, Sugiarti RM, Syafitri UD, Wahyuni WT, Rohaeti E. 2021. Ftir-based fingerprinting combined with chemometrics for discrimination of *Sonchus arvensis* leaf extracts and correlation with their antioxidant activity. Indones J Pharm 32 (2): 132-140. DOI: 10.22146/ijp.755.
Rasemi S, Yen KH, Ahmad R, Hasan MH. 2014. Total phenolic contents, antioxidants, anticancer and antidiabetic properties of *Myrmecodia tuberous* (Rubiaceae). Adv Chem Ser 9 (3): 2000-2004. DOI: 10.24297/jac.v9i3.1007.
Ratnadewi D, Umar AH, Sumaryono. 2023. Metabolit Sekunder Tumbuhan: Alternatif Produksi melalui Kultur In Vitro. IPB Press, Bogor. [Indonesian]
Raya MK, Legowo A, Wijayahadi N. 2016. The effectiveness of ant plant root extract (*Myrmecodia pendens* Merr.& Perry) as a decrease in blood glucose levels in *Sprague dawley* rats diabetes mellitus. J Gizi Indonesia 4 (2): 138-144. DOI: 10.14710/jgi.4.2.138-144. [Indonesian]
Salazar-Aranda R, Parez-Lopez L, Lopez-Arroyo, Alanis-Garza BA, Waksman de Torres N. 2009. Antimicrobial and antioxidant activities of plants from northeast of Mexico. e-CAM 41 (2): 233-236. DOI: 10.1093/ecam/nep127.
Sankhla MS, Parihar K, Kumar R, Bhagat D, Swaroop S, Sonone, Singh G, Nagar V, Awasthi G, Yadav CS. 2022. Ecofriendly approach for steroids, terpenes, and alkaloids-based biosurfactant. Biointerface Res Appl Chem 13 (2): 114. DOI: 10.33263/BRIAC132.114.
Sari YP. 2017. Short Communications: the potential of secondary metabolites of *Myrmecodia tuberous* from different host trees. Nusantara Biosci 9 (2): 170-174. DOI: 10.13057/nusbiosci/n090211.
Silalahi M, Nisyawati, Purba EC, Abinawanto DW, Wahyuningtyas RS. 2021. Ethnobotanical study of Zingiberaceae rhizomes as traditional medicine ingredients by medicinal plant traders in the Pancur Batu traditional market, North Sumatera, Indonesia. J Ethnobiol 4: 78-95. DOI: 10.46359/jte.v4i2.54.
Sulistyani M. 2018. Fourier transform infra red spectroscopy with reflectance method (ATR-FTIR) on optimization of vitamin C vibration spectrum measurements. J TEMAPELA 1(2): 39-43. DOI: 10.25077/temapela.1.2.39-43.2018. [Indonesian]
Umar AH, Ratnadewi D, Rafi M, Sulistyaningsih, Hamim H. 2021a. Metabolite profiling, distribution of secretory structures, and histochemistry in *Curculigo orchioides* Gaertn. and *Curculigo latifolia* Dryand. ex W.T.Aiton. Turk J Bot 45: 1-13. DOI: 10.3906/bot-2009-43.
Umar AH, Ratnadewi D, Rafi, M, Sulistyaningsih YC. 2021b. Untargeted metabolomics analysis using FTIR and UHPLC-Q-Orbitrap HRMS of two *Curculigo* species and evaluation of their antioxidant and α-glucosidase inhibitory activities. Metabolites 11 (42): 1-16. DOI: 10.3390/metabo11010042.
Utami RD, Zuhud EAM, Hikmat A. 2019. Medicinal ethnobotany and potential of medicine plants of Anak Rawa Ethnic at the Penyengat village sungai Apit Siak Riau. Media Konservasi 24: 40-51. DOI: 10.29244/medkon.24.1.40-51. [Indonesian]
Wang B, Wang J, Zhao X-H. 2022. Bioactivity of two polyphenols quercetin and fisetin against human gastric adenocarcinoma AGS cells as affected by two coexisting proteins. Molecules 27 (9): 2877. DOI: 10.3390/molecules27092877.
Yudthavorasit S, Wongravee K, Leepipatpiboon N. 2014. Characteristic fingerprint based on gingerol derivative analysis for discrimination of ginger (Zingiber officinale) according to geographical origin using HPLC-DAD combined with chemometrics. Food Chem. 158: 101–111.DOI: 10.1016/j.foodchem.2014.02.086.
Yuletnawati SE, Meiyanto E, Augustine D. 2013. High antitumor activity of ethanolic extracts of Papua's ant-plant (*Myrmecodia tuberosa*) on an oral carcinoma (kb) cell line. IJSR 6 (14): 2319-7064. DOI: 10.21275/v5i1.nov1531391.